

Superior Antitumor Efficacy of IFN- α 2b-Incorporated Photo-Cross-Linked Hydrogels Combined with T Cell Transfer and Low-Dose Irradiation Against Gastric Cancer

This article was published in the following Dove Press journal:
International Journal of Nanomedicine

Qin Liu^{1,*}
Dinghu Zhang^{1,2,*}
Hanqing Qian¹
Yanhong Chu¹
Yan Yang³
Jie Shao¹
Qiuping Xu¹
Baorui Liu¹

¹The Comprehensive Cancer Centre of Drum Tower Hospital, Medical School of Nanjing University, Clinical Cancer Institute of Nanjing University, Nanjing, People's Republic of China; ²Department of Radiology, Zhejiang Cancer Hospital, Hangzhou, People's Republic of China; ³Department of Oncology, Jiangning Hospital, Nanjing, People's Republic of China

*These authors contributed equally to this work

Introduction: The exhaustion and poor homing of activated lymphocytes are critical obstacles in adoptive cell immunotherapy for solid tumors. In order to effectively deliver immune cells into tumors, we encapsulated interferon- α 2b (IFN- α 2b) into macroporous hydrogels as an enhancement factor and utilized low-dose irradiation (LDI) as a tumoral attractor of T cells.

Methods: Hydroxypropyl cellulose hydrogels were prepared by irradiation techniques, and the cross-sectional microstructure was characterized by scanning electron microscopy. The synergistic antitumor mechanism of combination of IFN- α 2b and CIK cells was evaluated by detecting the expression of activation marker CD69 on CIK cell surface and IFN- γ production by CIK cells. The in vivo antitumor activity of IFN- α 2b-incorporated hydroxypropyl cellulose hydrogels combined with CIK and radiation was evaluated in an MKN-45 xenografted nude mice model.

Results: The bioactivity of IFN- α 2b was well maintained in ultraviolet-reactive, rapidly cross-linkable hydroxypropyl cellulose hydrogels. In vitro studies demonstrated IFN- α 2b-activated T cells, as evidenced by upregulating early activation marker CD69 and secretion inflammatory cytokine IFN- γ . In vivo real-time image showed our hydrogels kept a higher amount of drug delivery at the tumor site for a long time compared with free drug injection. Low-dose irradiation promoted T cell accumulation and infiltration in subcutaneous tumors. Combination of IFN- α 2b-loaded hydrogels (Gel-IFN) with T cells and LDI exhibited higher efficacy to eradicate human gastric cancer xenografted tumors with less proliferating cells and more necrotic regions compared with IFN- α 2b or T cells alone.

Discussion: HPC hydrogels kept the activity of IFN- α 2b and stably release of IFN- α 2b to stimulate T cells for a long time. At the same time, low-dose radiation recruits T cells into tumors. This innovative integration mode of IFN- α 2b-loaded hydrogels and radiotherapy offers a potent strategy to improve the therapeutic outcome of T cell therapy.

Keywords: gastric cancer, adoptive cell transfer, interferon- α 2b, hydrogels, low-dose irradiation

Correspondence: Baorui Liu
The Comprehensive Cancer Centre of Drum Tower Hospital, Medical School of Nanjing University, Clinical Cancer Institute of Nanjing University, Nanjing 210008, People's Republic of China
Tel +86 25-83107081
Fax +86 25-83317016
Email baoruilu@nju.edu.cn

Introduction

Advanced gastric cancer (GC) is a highly aggressive and life-threatening disease worldwide.¹ Various efforts have been made to improve curative effects, therapeutic responses are still limited. Immunotherapeutic strategies and clinical trials are currently under investigation. Recently, immune checkpoint inhibitors against

programmed cell death protein 1 (PD-1) exhibited an emerging opportunity and improved the survival time of GC patients.² However, only a minority of PD-L1-positive gastric cancer patients could benefit from PD-1 antibody during the clinical trial.³ Identification of possible predictive biomarkers and precise selection patients are still unsolved. Adoptive cellular therapy (ACT), another passive immunotherapeutic strategy,⁴ is based on the transfer of in vitro activated and expanded T cells into a tumor-bearing host to destruct malignancies. Chimeric antigen receptor T cells (CAR-T) exhibited impressive efficacy in hematological malignancies and raised the expectations of applying them in treating solid tumors.⁵ The disappointing results of CAR-T therapy against solid tumors were closely related to various obstacles,^{6,7} such as the lack of a unique tumor-restricted antigen, tumor heterogeneity, tumor immunosuppressive microenvironment, insufficient trafficking of CAR-T cells to tumor site. Moreover, CAR-T cell therapy might induce immune-related toxicity, namely, cytokine release syndrome and neurotoxicity.⁸

Cytokine-induced killer (CIK) cells, a heterogeneous subset of in vitro expanded T effector lymphocytes, presented major histocompatibility complex-unrestricted tumor-killing ability.^{9,10} CIK cell-based clinical studies demonstrated a great promise in solid tumor treatment. Autologous transplantation of CIK cells as an adjuvant therapy increased the disease-free survival (DFS) of patients with hepatocellular carcinoma after surgical resection.¹¹ CIK cells were also reported to prolong overall survival without serious adverse events for patients with advanced gastric cancer.¹² The noticeable challenge in the clinical translation of CIK cells was how to efficiently traffic T cells into tumor sites and keep their in vivo persistent activity following adoptive transfer.

IFN- α has been approved for the management of several neoplastic diseases.¹³ IFN- α can prolong disease-free survival and overall survival for stage II & III melanoma patients.¹⁴ Besides direct antitumor activity, IFN- α pleiotropically affects immune response by modulating the activation and proliferation of immunocytes.¹⁵ IFN- α also favors the differentiation of naive CD4⁺ T cells into Th1-like T cells and increases IFN- γ production of CD8⁺ T cells.¹⁶ However, systemic administration of IFN- α usually induces severe events with half of patients who require drug withdrawal or dose reduction. The clinical use of IFN- α was restricted by short terminal half-life, rapid peripheral blood-mediated proteolysis as well as hepatic and renal clearance.¹⁷ Local administration of low-dose IFN-

α showed high antitumor activity through inducing high affinity between immune effector cells and tumor cells. However, repeated intratumoral injections might induce discomfort for patients and increase the frequency of clinical visits.

Local implantation of hydrogels offers an effective delivery of protein/DNA to the targeted tissues in a safe, controlled, and patient-friendly manner.^{18,19} On the other hand, ionizing radiation not only can induce tissue damage, inflammation, but also trigger antitumor immune immunity.^{20,21} The impacts of radiotherapy on the innate and adaptive immune system depend on radiation dose, fraction and combined mode.^{22,23} Low-dose irradiation (LDI) caused aberrant vascular normalization and induced the highest ratio of effector T cells to immunosuppressive regulatory T cells when combined with adoptive T cell transfer.²⁴ Our previous study also reported that 2 Gy LDI enhanced the efficacy of adoptive T lymphocytes against gastric cancer cells through recruitment cytotoxic T cells at the tumor sites.²⁵

From the above perspectives, we here described a novel strategy by utilizing a simple ultraviolet (UV) light-reactive, rapidly cross-linkable and biodegradable hydrogels to sustain release IFN- α 2b (Figure 1). LDI was used to increase the accumulation of T cells in tumor regions. The anticancer efficacy of combining IFN- α 2b with hydrogels (Gel-IFN), intraperitoneal administration of T cells, and LDI was explored on a gastric cancer xenografted mice model.

Materials and Methods

Cell Lines and Materials

All the experimental methods and the blood collection procedure were carried out in accordance with the guidelines approved by the Ethics Committee of Nanjing Drum Tower Hospital. One gastric patient agreed to donate blood samples and signed a written informed consent form for scientific research and clinical development of new technologies without prejudice to diagnosis, clinical testing and treatment for him. We kept our pledge to protect the privacy of patients. The human gastric cancer cell line MKN-45 and human melanoma cell line A375 (Shanghai Institute of Cell Biology, China) were cultured in RPMI 1640 medium, supplemented with 10% fetal bovine serum, 50 IU/mL penicillin and 50 mg/mL streptomycin sulfate with 5% CO₂ at 37°C. Hydroxypropyl cellulose (HPC, Mn = 100 kDa) was purchased from Alfa Aesar (Shanghai, China). Human IFN- α 2b was supplied by Merck

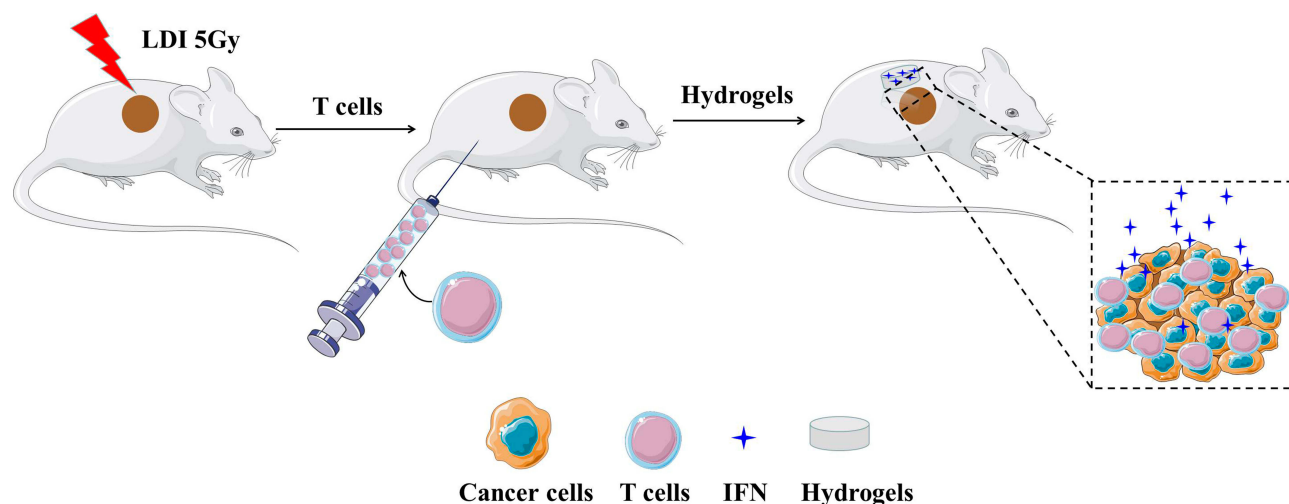


Figure 1 The schematic diagram for the enhanced intratumor delivery of T cells by IFN- α 2b-loaded hydrogels and low-dose irradiation (LDI). Tumor tissues of nude mice were treated with radiotherapy on day 1. T cells were injected intraperitoneally on day 2, and hydrogels loaded with IFN- α 2b was implanted subcutaneously on day 3. **Abbreviations:** IFN, interferon; LDI, low-dose irradiation.

Sharp & Dohme (Germany). 3-[4, 5-Dimethyl-2-thiazolyl]-2, 5-diphenyl-2H-tetrazolium bromide (MTT), *N,N*-dicyclohexylcarbodiimide (DCC), 4-dimethylaminopyridine (DMAP), methacrylic anhydride (MA) and 2-hydroxy-1-[4-(2-hydroxyethoxy)phenyl]-2-methyl-1-propanone (I2959) were purchased from Shanghai Aladdin (China). Near-infrared-797 (NIR-797) was obtained from Sigma-Aldrich (USA).

Preparation of IFN- α 2b-Loaded Hydrogels (Gel-IFN)

The HPC hydrogels were synthesized by an ultraviolet light-reactive, rapidly cross-linkable method as previously described.²⁶ Briefly, 0.63 mL MA, 0.4 g DMAP and 0.86 g DCC were added dropwise in HPC (8.0 g) dissolved in chloroform (3.0 mL). The final mixtures were obtained by concentrating and precipitating the solution with diethyl ether. The polymer was then dissolved in water, filtered, dialyzed for 72 h and lyophilized. Afterwards, the lyophilizate was dissolved in deionized water at 20% (w/v), followed by a photoinitiator I2959 at a concentration of 4% (w/w) of the lyophilizate weight. Each well of 96-well plates was filled with 50 μ L of the solution, which was then cross-linked with UV light (365~400 nm, 125w) at a distance of approximately 20 cm using an UV cross-linker (Ausbond, China) for 7 min. Finally, the cross-linked gels were washed with deionized water, freeze-dried and stored at room temperature. The resulting hydrogel was a cylindrical structure with a diameter of 6.4mm and a height of 1.6mm. The cross-sectional microstructure was characterized by scanning electron microscopy (SEM, JSM-

5410LV, JEOL, Japan) and the average pores' diameters of HPC hydrogels were calculated. IFN- α 2b was diluted with PBS to obtain different concentrations (2×10^3 , 1×10^4 , 2×10^4 IU/mL) and added on the surface of the HPC hydrogels. The hydrogels were then placed at 4°C overnight to allow the IFN- α 2b to sufficiently permeate the gel.

In vitro Release of IFN- α 2b from Gel-IFN

To determine the release kinetics of IFN- α 2b from HPC hydrogels, Gel-IFN (IFN- α 2b: 3×10^5 IU/mL) were incubated in sterile PBS at 37°C. PBS release medium were withdrawn at the appointed time and replaced with the same amount of fresh phosphate-buffered saline (PBS). IFN- α 2b in the supernatant was detected using a human IFN- α enzyme-linked immunosorbent assay (ELISA, Mabtech, Sweden) according to the manufacturer's protocol and stored at -20°C until further analysis.

Isolation and Culture of Primary Human T Lymphocytes

Peripheral blood mononuclear cells (PBMCs) from donor gastric cancer patients were isolated by a Ficoll density gradient centrifugation, and then resuspended in AIM-V medium containing 10% fetal bovine serum at a concentration of 1.5×10^6 cells/mL. PBMCs were treated with IFN- γ (1000 IU/mL) and anti-CD3 antibody (50 ng/mL) for 24 hours. Fresh IL-2 (0.300U/mL) was added and replaced every 2 to 3 days. T cells were incubated for three weeks.

In vitro Cytotoxicity of IFN- α 2b and T Cells on Gastric Cancer Cells

Human gastric carcinoma MKN-45 cells were seeded in 96-well plates (5000/well) for 24h. Then, cells were treated with various concentrations of IFN- α 2b (1000, 5000, 10,000 IU/mL) and T cells at different Effect:Target (E:T) ratios of 5:1, 10:1, 20:1 and 40:1 for 12 hours. After removing the media, the culture plates were rinsed thrice in the media. The cytotoxic activity was measured by MTT assay, and the optical density (OD) was read on a microplate reader at 490 nm wavelength. We calculated the cell viability according to the following equation:

$$\text{Cell viability (\%)} = \frac{\text{OD of test group} - \text{OD of blank group}}{\text{OD of control group} - \text{OD of blank group}} \times 100\%$$

The combining of IFN- α 2b with T cells on gastric cancer cells' inhibition was also assessed as described above.

CD69 and IFN- γ Expressions

After the 5×10^5 T cells were treated with IFN- α 2b (1,000 IU/mL) or PBS solution for 12 hours, the supernatants were obtained by centrifuging the T cells for 5 minutes at 1,000 r/min and used for analysis of IFN- γ expression by BD™ CBA Human IFN- γ flex set (BD Bioscience). The T cells were harvested and stained with fluorescent-labeled mouse anti-human antibody CD3-PerCP-Cy5.5 and CD69-PE (BD Bioscience).

In vivo Antitumor Effect of Gel-IFN Combined with T Cells and LDI

BALB/c nude mice (male, 5–6 weeks) were supplied by the department of Yangzhou University experimental animals (Yangzhou, China). All animal experiments were performed in accordance with the guidelines verified and approved by the Ethics Committee of Drum Tower Hospital. BALB/c nude mice were inoculated subcutaneously with 1×10^6 MKN-45 cells. When the tumors reached an average volume of 200 mm³, the mice were randomized into five groups (5 mice per group) as follows: (a) Normal saline group. (b) IFN- α 2b group. (c) T cells + LDI group. (d) IFN- α 2b + T cells + LDI group. (e) Gel-IFN + T cells + LDI group. Radiation was administered at a dose of 5 Gy using a 6-MeV electron beam on day 1 and 5×10^6 T cells were intraperitoneally transferred in 200 μ L saline on day 2. Gel-IFN or equal amount of IFN- α 2b (6×10^5 IU) were subcutaneously implanted into mice on day 3. The sites of Gel-IFN implantation and IFN- α 2b injection were

located subcutaneously at a 5 mm distance to the tumors. Tumor volumes were calculated according to the formula: volumes = 0.5 \times length \times width². Tumor volumes were measured simultaneously every other day. Mice were sacrificed by cervical dislocation on day 13. The tumor inhibition rate = (1-experimental group volume /control group volume) \times 100%. Tumors were collected for tumor weighting and processed routinely into paraffin for hematoxylin and eosin (H&E) staining.

In vivo Real-Time Imaging

All animal studies were performed in compliance with guidelines set by the animal Care Committee at Drum Tower Hospital, Nanjing, China. When the tumors reached an average volume of 200 mm³, NIR-797 (1 mg/mL)-loaded HPC hydrogels or free NIR-797 were subcutaneously administered into MKN-45 gastric tumor-bearing mice, respectively. The real-time biodistribution of NIR-797 formations was investigated by the IVIS® Lumina system (Xenogen Co, Alameda, CA, USA) at selected time points. The fluorescence at 745 nm was collected and the exposure time was set to 2 seconds.

T Cell Infiltration in the Tumors

BALB/c nude mice were inoculated subcutaneously with 1×10^6 MKN-45 cells. When the tumors reached about 200 mm³ in volume, mice received either 5 Gy local tumor irradiation. After 24 hours, mice were intraperitoneally injected with 5×10^6 T cells. One day later, tumors were excised and fixed in 4% formaldehyde, embedded in paraffin wax. Primary antibody rabbit anti-human CD3 antibody and secondary antibody anti-rabbit HRP conjugate (Abcam, UK) were used for immunohistochemistry staining.

Statistical Analysis

Data are expressed as mean \pm standard deviation. Differences between the values were assessed using one-way ANOVA and Student's *t*-test, while $P < 0.05$ was considered statistically significant.

Results

Characterization of HPC Hydrogels

Hydrogel implants, three-dimensional polymeric networks swollen in water aqueous media or biological/physiological fluids, have shown certain prolonged tumor drug exposure and sustained drug release as well as reduced systemic toxicity.²⁷ Biocompatible and biodegradable hydrogels can

sustain release inflammatory signals and adjuvants, recruit dendritic cells and subsequent homing to lymph nodes.^{28,29} HPC, the most abundant renewable polysaccharide in nature, has been approved by the Food and Drug Administration (FDA) as drug delivery substrate.³⁰ In this study, we prepared HPC hydrogels by an easy irradiation technique for controlled protein release. The HPC hydrogels exhibited a porous structure, consisting of open pore channels and an interconnected framework (Figure 2A). Most of these pores had an approximately cylindrical microstructure with an average pore diameter of $\sim 10\ \mu\text{m}$, allowing IFN- $\alpha 2\text{b}$ to diffuse freely within the gel matrix. Figure 2B shows the accumulative diffusion profiles of IFN- $\alpha 2\text{b}$ through the HPC hydrogels. Approximately 50% of the encapsulated IFN- $\alpha 2\text{b}$ was released within the first 5 hours. The burst pattern might originate from IFN- $\alpha 2\text{b}$ abrupt release of the exposed drug on the surface of the hydrogels. Subsequently, IFN- $\alpha 2\text{b}$ release from the hydrogels continued at a much slower release rate for a long period through diffusion mechanism from the porous network. We found that $80.91 \pm 3.75\%$ of IFN- $\alpha 2\text{b}$ were released from HPC hydrogels in the first 24 hours. Ninety percent protein could be released from HPC hydrogels by diffusion mechanism within 120 hours without full degradation of hydrogels.

Effects of IFN- $\alpha 2\text{b}$ on the Activity T Cells

We then evaluated the cytotoxicity of IFN- $\alpha 2\text{b}$ and different E:T ratios of T cells on gastric cancer cells. It was found that $89.23 \pm 3.4\%$ cancer cells were still alive when

treated with IFN- $\alpha 2\text{b}$ at a final concentration of 10,000 IU/mL, indicating slight antitumor activity of IFN- $\alpha 2\text{b}$ (Figure 3A). On the other hand, T cells exerted their cytotoxicity against gastric cancer cells in a typically E:T ratio-dependent manner (Figure 3B). When the ratios of E:T were 0:1, 5:1, 10:1 and 20:1, the cytotoxicity of T cells against MKN-45 cell line was $100.00 \pm 9.00\%$, $90.87 \pm 4.00\%$, $85.87 \pm 9.00\%$ and $76.27 \pm 10.00\%$, respectively. The 20:1 E:t ratio was used in the following cytotoxicity experiments. Results showed that IFN- $\alpha 2\text{b}$ + T cells and Gel-IFN + T cells significantly induced an increase of MKN-45 cell line suppression by $66.66 \pm 4.08\%$ and $69.00 \pm 4.41\%$ versus T cells alone, respectively ($P < 0.01$, Figure 3C). In addition, blank hydrogels did not suppress proliferation of tumor cells, indicating the hydrogels itself was non-toxic to cells. For Gel-IFN, a high activity of IFN- $\alpha 2\text{b}$ was maintained.

To better understand the synergistic antitumor mechanism of IFN- $\alpha 2\text{b}$ and T cells, we examined the expression of activation marker CD69 on T cell surface and IFN- γ level secretion by T cells. After treated with IFN- $\alpha 2\text{b}$, the percentages of $\text{CD}3^+\text{CD}69^+$ T cells increased as compared to the control (44.6% VS 34.4%, Figure 4A), indicating IFN- α induced active T lymphocytes. IFN- γ was originally called immune cells-activating factor and played an important role in regulating antitumor immunity. We measured IFN- γ levels at 12 hours and found that IFN- $\alpha 2\text{b}$ significantly enhanced the expression of T cells treated, compared with T cells alone without adding IFN- $\alpha 2\text{b}$ ($P < 0.05$) (Figure 4B).

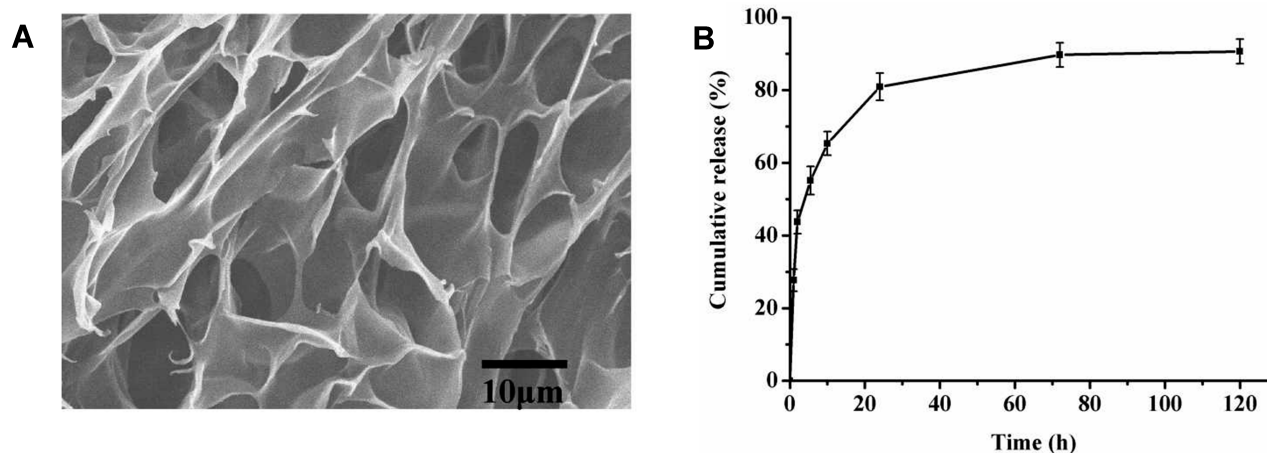


Figure 2 Characterization of HPC hydrogels. (A) The cross-sectional SEM micrographs of the hydrogels. (B) Cumulative release of IFN- $\alpha 2\text{b}$ from the hydrogels over a period of 120 hours in vitro.

Abbreviations: HPC, hydroxypropyl cellulose; SEM, scanning electron microscope; IFN, interferon.

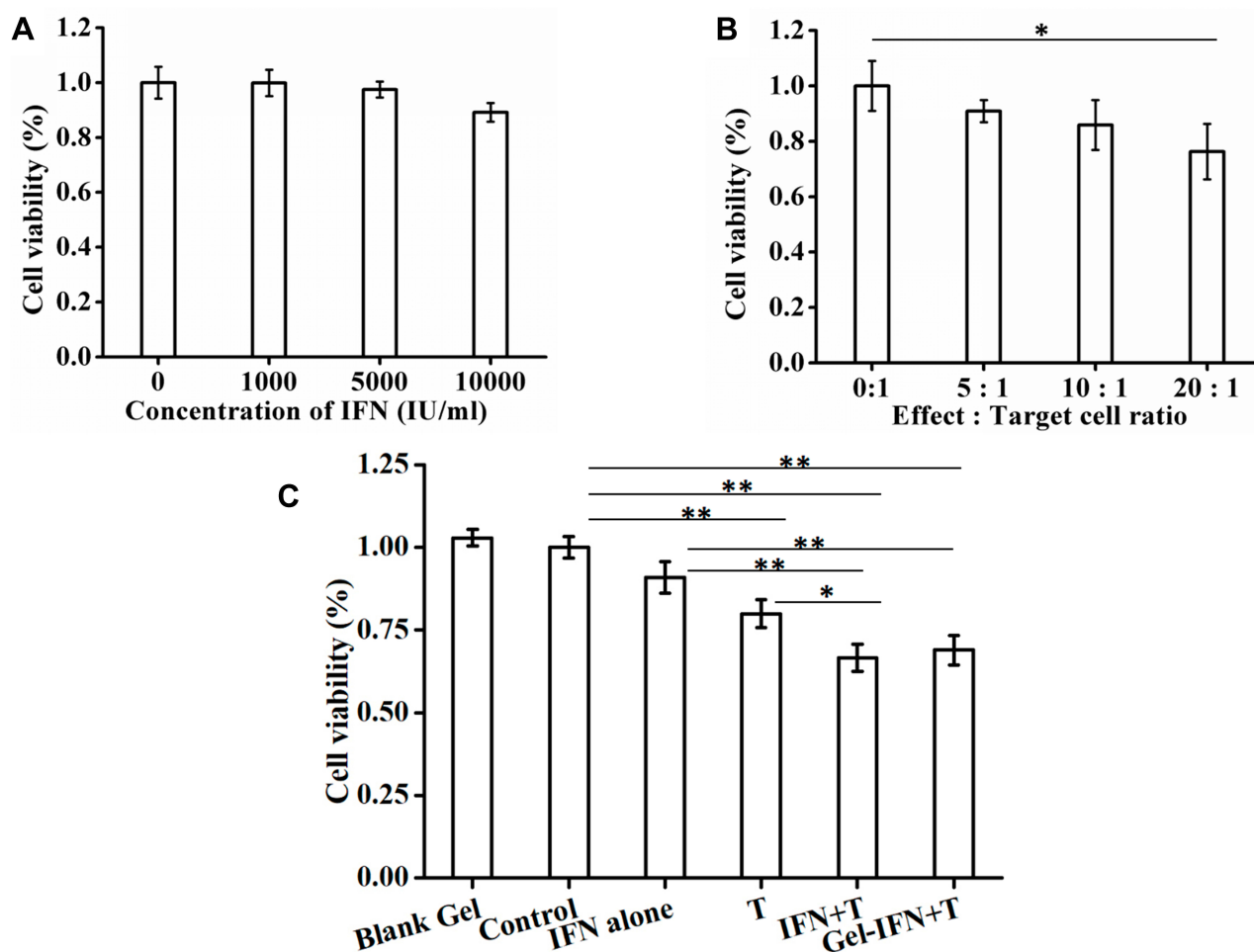


Figure 3 (A, B) Cell viability of MKN-45 gastric cancer cells after incubation with different concentrations of IFN- α 2b and different E:T ratios of T cells, respectively. **(C)** The cytotoxicity of IFN- α 2b, T cells, LDI and Gel-IFN + T cells + LDI against MKN-45 gastric cancer cells (* $P < 0.05$, ** $P < 0.01$). **Abbreviations:** IFN, interferon; E:T, Effect:Target; LDI, low-dose irradiation.

In vivo Real-Time Imaging

The drug-incorporated hydrogels can continuously release payloads on tumors and other tumor-draining sites to keep high local drug concentration. Previous studies have documented that the IFN- α -incorporated polymer could deliver agents to the tumor microenvironment and improved the antitumor effect against liver cancer.³¹ During our study, in vivo real-time biodistribution of drug in HPC hydrogels was examined through a non-invasive near-infrared fluorescence imaging by encapsulating a near-infrared fluorescent dye NIR-797 in the hydrogels. After Gel-dye or free NIR-dye was subcutaneously injected, mice were scanned at 1h, 3h, 24h, 48h, 72h and 120h to obtain the NIR fluorescence signals and observe the in vivo distribution of different dye formations. There was a similar fluorescence intensity in the Gel-dye group and free NIR group during the first one hour after administration (Figure 5A). As time went on, the

fluorescence intensity gradually decreased. The signals from free dye weaken more rapidly than Gel-dye formation. Few fluorescence signals from free NIR-797 could be detectable in the mice treated with free NIR-797 post 48 h injection. The fluorescence signals of tumor regions treated by the Gel group were always stronger than the signals of the free dye group during the whole 120 hours, suggesting that hydrogels preferred to concentrate and retain payloads in the tumor regions.

Local LDI Induces Infiltrating T Cells into Tumor Sites Retards Tumor Growth in vivo

The effectiveness of immunotherapies is mostly based on facilitating T cell trafficking into solid tumors for a variety of cancers. Gastric carcinoma MKN-45 bearing mice received a single dose of 5 Gy radiation, and then 5 \times

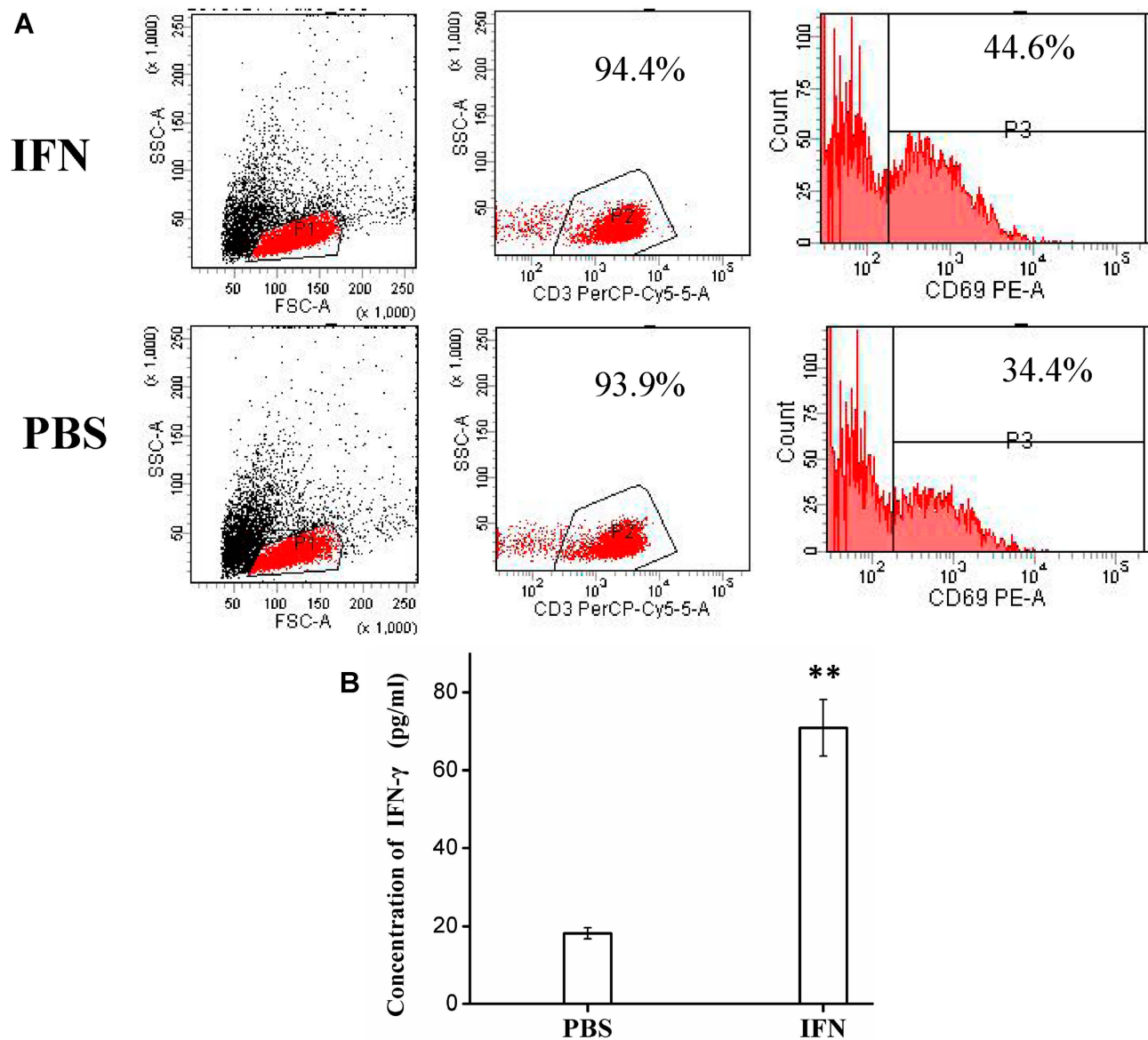


Figure 4 (A) Flow cytometry detection of CD69⁺ T cells in PBS and IFN- α 2b groups. **(B)** The IFN- γ expression of T cells when treated with IFN- α 2b (1,000 IU/mL) or PBS solution for 12 h. Data are expressed as mean \pm SD through three independent experiments (** $P < 0.01$).

Abbreviations: IFN, interferon; PBS, phosphate-buffered saline; FSC-A, forward scatter area; SSC-A, side scatter area; CD3, cluster of differentiation.

10^6 T cells were intraperitoneally transferred into mice 24 hours later. As showed in [Figure 5B](#), CD3⁺ T cells strongly accumulated to irradiated tumors, but T cells scarcely immigrated into unirradiated tumors, indicating local LDI promotes the recruitment of immune cells to established tumors.

Anticancer Effect in Gastric Cancer Xenografted Nude Mice

To explore the *in vivo* antitumor efficacy of different IFN- α 2b formulations and different integrating strategies, the mice subcutaneously implanted with human gastric cancer

MKN-45 was used as mice model. Mice treated with PBS or T cells were used as controls. The tumor inhibition rate of IFN- α 2b alone, T cells+ LDI, IFN- α 2b + T cells+ LDI and Gel-IFN + T cells+ LDI groups were 11.7%, 24.7%, 43.4% and 59.0%, respectively ([Figure 6A](#)). The tumor weight inhibition rates of IFN- α 2b alone, T cells + LDI, IFN- α 2b + T cells + LDI and Gel-IFN + T cells + LDI groups were 4.7%, 15.8%, 33.0% and 48.0%, respectively. IFN- α 2b + T cells + LDI significantly inhibited tumor volume and reduced tumor weight compared with the control group or free IFN- α 2b group ($P < 0.01$, [Figure 6B](#)). More importantly, Gel-IFN + T cells + LDI group exhibited a higher antitumor

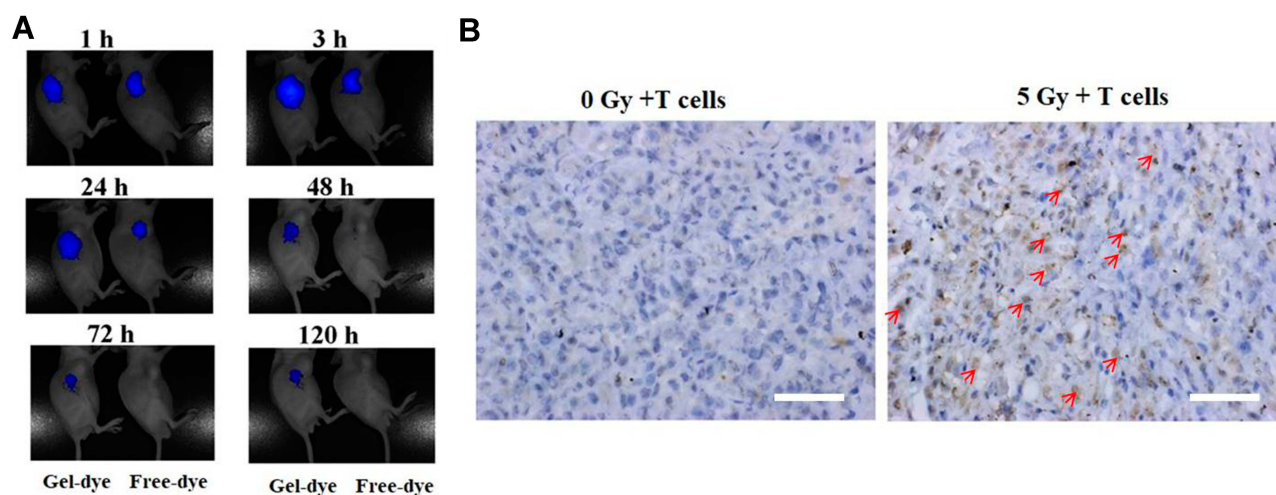


Figure 5 (A) In vivo real-time imaging of NIR-797-loaded HPC hydrogels (Gel-dye, left mice) or free NIR-797 (right mice) in tumor sites following subcutaneous administration. Fluorescence of NIR-797 was determined at different time points. **(B)** Tumor infiltration of T cells following a single local dose of 5 Gy irradiation. The red arrows indicated the T cells. Scale bar = 50µm.

Abbreviation: HPC, hydroxypropyl cellulose.

effect compared with the T cells + LDI group ($P < 0.05$). Figure 6C shows the photo of excised tumors from each treatment group. The tumor volumes of mice treated by Gel-IFN + T cells + LDI were smallest. T lymphocyte recruitment also depends on functional vasculature improvement. Abnormal tumor vasculatures could not sustain tumor perfusion and adequate blood flow, thus induced hypoxia and immunosuppression, thus limiting drug and immune cell access. Preclinical studies demonstrated that the therapeutic value of vascular normalization in immune checkpoint therapy.³² Combinations of anti-angiogenesis drugs with immune checkpoint inhibitors have become an attractive strategy. LDI was also verified to improve tumor vessel function and immune rejection. In the following study, we will explore further mechanisms such as vessel normalization and hypoxia profile, which may contribute to the tumor volume reduction.

To investigate the mechanisms behind the potent antitumor effects, we performed histological changes of tumor tissues for the mice treated with different groups. Figure 6D shows the hematoxylin and eosin (H&E) staining of the excised tumors treated with normal saline, IFN- α 2b, LDI + T cells, LDI + T cells + IFN or LDI + T cells + Gel-IFN after 13rd day post-injection. The numbers of living tumor cells in LDI + T cells + Gel-IFN-treated group was much lower than that of other groups. On the contrary, the area of necrotic region in the tumors from the mice treated with the hydrogel formulations was large, which was consistent with the tumor regression results.

Discussions

Adoptive cell transfer therapy has been proved as a promising tool in the scenario of cancer immunotherapeutic strategies. CIK cells are a subset of ex-vivo expanded effector T lymphocytes which are endowed with a non-major histocompatibility complex (MHC) restricted anti-tumor activity, allowing inhibiting the heterogeneous tumor cell populations.^{9,10} However, some major challenges, such as “on-target/off-tumor” toxicity, cytokine release syndrome as well as inadequate T cell migration across the tumor physical and biochemical barriers are usually the bottleneck associated with adoptive immune cell therapy in solid tumors.³³ Besides, T cells also undergo apoptosis and exhaustion with no increase in potential antitumor cells. The low response rate of adoptive cell emphasized the need to develop new strategies to increase its efficacy. It is reported that the combination of T cells with cytokines or other strategies broad the application of T cells immunotherapy in the clinic. Oliso et al reported the results of their clinical trial about cytokine-induced killer cells in solid and hematopoietic tumours.³⁴ Two metastatic hepatocellular carcinoma patients reached complete response when they received CIK cells treatment and the simultaneous subcutaneous injection of low-dose IL-2 and IFN- α , respectively.

IFN- α , a cytokine has shown antitumoral activity in murine tumor models including gastric carcinoma, is sufficient to induce mature lymphocytes. IFN- α also plays an important role in mediating the functional changes in lymphocytes.

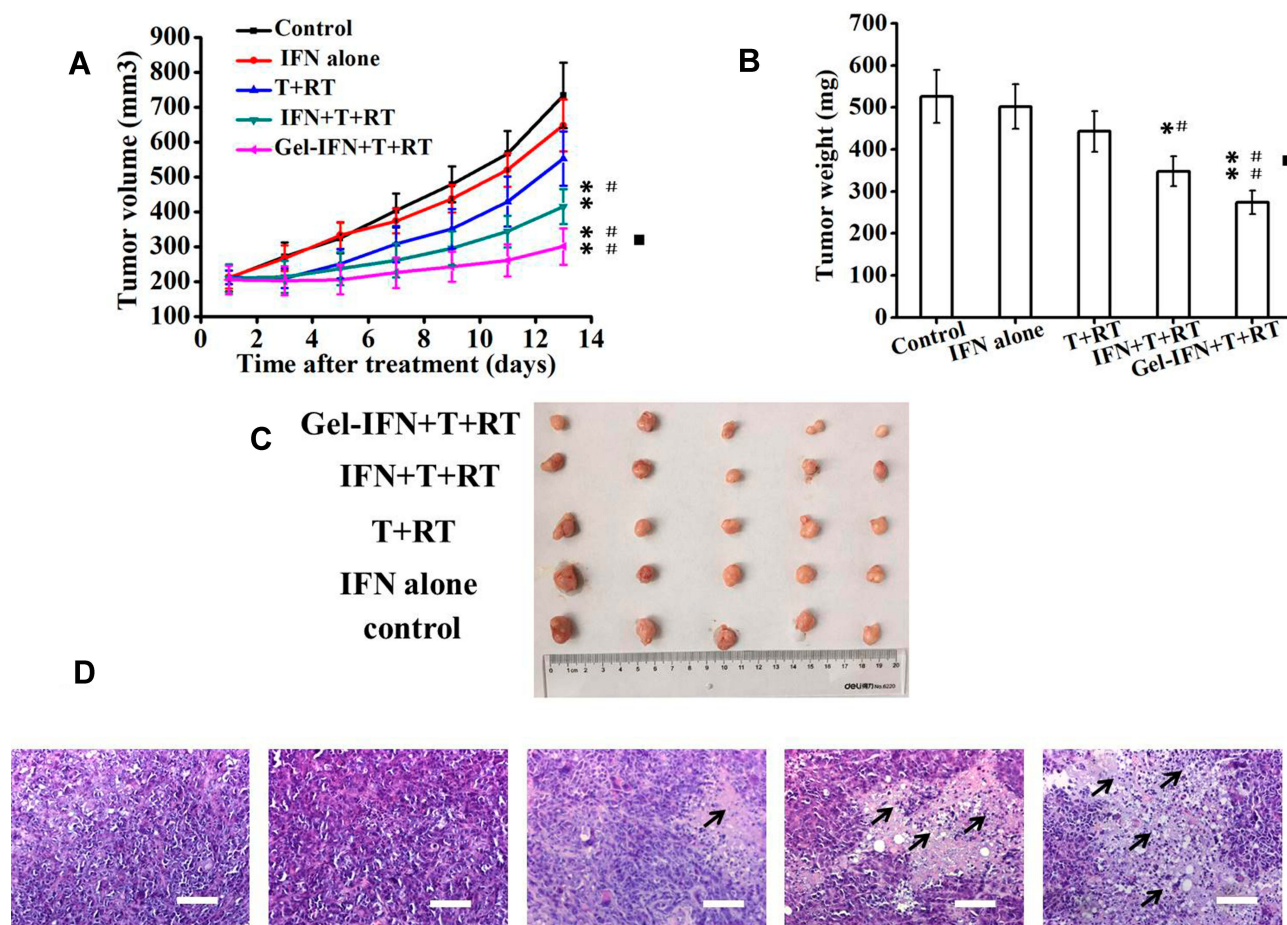


Figure 6 In vivo antitumor efficacy of Gel-IFN + T cells + LDI on BALB/c nude mice bearing MKN-45 gastric cancer cells. When the tumors reached an average volume of 200 mm³, the mice were randomized into five groups as follows: (1) Control (normal saline), (2) IFN- α 2b alone (6×10^5 IU, subcutaneous injection, day 3), (3) LDI (5 Gy, day 1) + T cells (5×10^6 cells, day 2), (4) LDI + T cells + IFN- α 2b, (5) LDI + T cells + Gel-IFN (subcutaneous implantation). **(A)** Inhibition of MKN-45 xenograft tumor growth by LDI + T cells + Gel-IFN in comparison with various formulations. **(B)** The tumor weights on day 13 following different treatments. **(C)** The tumor photographs of different groups. **(D)** H&E staining of tumors after anticancer treatments (magnification: 200 \times). Data are expressed as mean \pm SD (n=5), *P < 0.05 and **P < 0.01 versus control group, #P < 0.05 and ##P < 0.01 versus free IFN- α 2b group, *P < 0.05 versus LDI + T cells group. The black arrows indicated the necrosis area. Scale bar = 100 μ m.

Abbreviations: IFN, interferon; T, thymus; RT, radiation; LDI, low-dose irradiation; H&E, hematoxylin–eosin.

However, non-selective administration of IFN usually induced normal organs injury and other undesired adverse effects. IFN- α 2b was also hampered owing to short circulation time and instability under room temperature. Besides, repeated injection of IFN- α is costly and inconvenient. Pegylated IFN- α 2b was approved by the FDA in 2001 for its long circulation and decreasing breakdown. But the cost was high and side effects are clinical obstacles. To address these limitations, a biocompatible and biodegradable implanting hydrogel was prepared in this present study to sustained release and prolong retention of IFN- α 2b. Hydrogels can be delivered in a minimally invasive manner, provide sustained release of immunomodulators and bypass the need for genetic modification of transplanted cancer cells.

Among various kinds of hydrogels, photocrosslinked hydrogels have been developed for drug delivery with

highly tunable biochemical and biophysical properties in both the spatial and temporal scales.^{35–37} Hydrogels based on hydroxypropyl cellulose (HPC) have attracted intense attention due to several advantages of HPC such as the commercial derivative of cellulose, the abundant renewable resource, no cytotoxicity and approval by the Food and Drug Administration (FDA).³⁰ The photocrosslinked HPC hydrogels have been developed as a biocompatibility substrate for cell sheet engineering.²⁶ In this study, their role was extended to serve as a vehicle for drug delivery. HPC hydrogels provided high pore volume and large surface area for controlled drug release. IFN- α 2b, which was released from HPC hydrogels constitutively activated immunocytes. IFN-Gel or free IFN- α 2b induced IFN- γ secretion in the T cells in vitro, suggesting a response due to stimulating

cytokines. In vitro cytotoxicity showed IFN-Gel could suppress tumor cells. Concerning the sustained release of hydrogel formations, less than 50% IFN release from hydrogels in 12 hours, the cytotoxicity of Gel-IFN is higher than free IFN in fact. Macroporous hydrogels could present payloads in a sustained and localized manner. In vivo real-time near-infrared imaging demonstrated that hydrogels, compared with free dyes, obviously prolonged fluorescence dye retention nearby the tumor regions (Figure 5A). Concentration and retention are important for ideal therapeutic efficiency. Additionally, the treatment with blank hydrogels exerted no observable toxicity.

An important barrier for adoptive cell transfer is the poor homing of immunocyte cells to tumors.³⁸ Chan et al verified that T cells conjugated with bispecific antibodies against CA125 and Her2 showed significantly in vivo activity against CA125- and Her-2-expressed tumors.³⁹ Zou et al reported that T cells modified with folate receptor improved antitumor immunity of T cells.⁴⁰ Radiation, an important type of local therapy in advanced gastric cancer, has been reported to potentiate the efficacy of immunotherapy. Klug et al demonstrated LDI promoted normalization of aberrant vasculature and immune cell infiltration in the tumor microenvironment.²⁴ According to data from orthotopic pancreatic tumors, LDI increased the ratio of active immune cells to immunosuppressive cells through upgrading CD4+ T cell infiltration and decreasing Treg cells. They irradiated established tumors with a single dose of 2Gy, and 1 day later, mice were intravenously injected with T cells. As a result, the combination of LDI and subsequent T cells transfer favored tumor suppression and prolonged the survival time of tumor-bearing mice. But, radiotherapy or T cell transfer alone did not inhibit tumor growth. Our previous study also showed 2Gy tumor irradiation improved the therapeutic efficacy of adoptive cellular immunotherapy for gastric tumor-bearing mice.²⁵ Based on the above experimental results, we firstly administered radiation for the tumor tissue and then delivered T cells one day later, with the goal of recruiting T cells to the tumor tissue. Finally, we gave the IFN-Gel to fully activate T cells in tumor tissues by using the slow-release property of hydrogels. In this present study, LDI also increased the in vivo recruitment of cytotoxic T lymphocytes to tumor tissues. A number of CD3+ T cells were observed in LDI treated tumors, in contrast to

radiation-free tumors. As a result, IFN-Gel combined with LDI and T cells showed the strongest antitumor activity. Extensive tumor suppression by IFN-Gel, LDI and T cells was further confirmed by histological evaluation of tumors at two weeks after treatment, showing that the synergistic effect.

All these efforts promoted the development and evolution of T cell-based therapy and moved towards our ultimate goal-curing cancer with high safety, high efficacy, and low cost. Needless to say, this new integrated treatment strategy combining with other therapeutic strategies, such as immune checkpoint inhibitors, antiangiogenic therapy and chemotherapy could be considered for increase therapeutic success.

Conclusions

In summary, our findings verified that IFN- α 2b-loaded hydrogels could sensitize T cells against gastric cancer cells by increasing the activity and IFN- γ production. HPC hydrogels kept the activity of IFN- α 2b and stably release of IFN- α 2b to stimulate T cells for a long time. At the same time, low-dose radiation recruits T cells into tumors. Our study illustrated a broader applicability based on T cells, an implantable hydrogel and low-dose radiation. We expected this kind of cancer comprehensive strategy could improve the anticancer effects of T cells on gastric cancer.

Acknowledgments

This work was supported by the National Natural Science Foundation of China (No. 81972309), Jiangsu Provincial Medical Youth Talent (No. QNRC2016045), Fundamental Research Funds for the Central Universities (No. 14380451) and the Nanjing Medical Health Science and Technology Development Fund (No. YKK18201).

Disclosure

The authors report no conflicts of interest in this work. The abstract of this paper was presented at the ESMO Asia 2018 Conference name “Superior antitumor efficacy of interferon-incorporated hydrogels combined with CIK and radiation against gastric cancer” as a poster presentation with interim findings. The poster’s abstract was published in “Poster Abstracts” in *Annals of Oncology*. 2018;29(s9) (<https://oncologypro.esmo.org/meeting-resources/esmo-asia-2018-congress/Superior-antitumor-efficacy-of-interferon-incorporated-hydrogels-combined-with-CIK-and-radiation-against-gastric-cancer>).

References

- Allemani C, Matsuda T, Di Carlo V, et al. Global surveillance of trends in cancer survival 2000-14 (CONCORD-3): analysis of individual records for 37 513 025 patients diagnosed with one of 18 cancers from 322 population-based registries in 71 countries. *Lancet*. 2018;391(10125):1023–1075. doi:10.1016/S0140-6736(17)33326-3
- Kang YK, Boku N, Satoh T, et al. Nivolumab in patients with advanced gastric or gastro-oesophageal junction cancer refractory to, or intolerant of, at least two previous chemotherapy regimens (ONO-4538-12, ATTRACTION-2): a randomised, double-blind, placebo-controlled, phase 3 trial. *Lancet*. 2017;390(10111):2461–2471. doi:10.1016/S0140-6736(17)31827-5
- Muro K, Chung HC, Shankaran V, et al. Pembrolizumab for patients with PD-L1-positive advanced gastric cancer (KEYNOTE-012): a multicentre, open-label, phase 1b trial. *Lancet Oncol*. 2016;17(6):717–726. doi:10.1016/S1470-2045(16)00175-3
- Wang M, Yin B, Wang HY, Wang RF. Current advances in T-cell-based cancer immunotherapy. *Immunotherapy*. 2014;6(12):1265–1278. doi:10.2217/imt.14.86
- Riviere I, Sadelain M. Chimeric antigen receptors: a cell and gene therapy perspective. *Mol Ther*. 2017;25(5):1117–1124. doi:10.1016/j.yimthe.2017.03.034
- Newick K, O'Brien S, Moon E, Albelda SM. CAR T cell therapy for solid tumors. *Annu Rev Med*. 2017;68(1):139–152. doi:10.1146/annurev-med-062315-120245
- Mirzaei HR, Rodriguez R, Shepphird J, et al. Chimeric antigen receptors t cell therapy in solid tumor: challenges and clinical applications. *Front Immunol*. 2017;8:1850. doi:10.3389/fimmu.2017.01850
- Neelapu SS, Tummala S, Kebriaei P, et al. Chimeric antigen receptor T-cell therapy - assessment and management of toxicities. *Nat Rev Clin Oncol*. 2018;15(1):47–62. doi:10.1038/nrcclinonc.2017.148
- Zhang L, Xu Z, Chen X, et al. Clinical benefits of Livin peptide-loaded DCs/CIKs combined with chemotherapy in advanced non-small cell lung cancer. *Am J Cancer Res*. 2019;9(2):406–414.
- Zhang L, Mu Y, Zhang A, et al. Cytokine-induced killer cells/dendritic cells-cytokine induced killer cells immunotherapy combined with chemotherapy for treatment of colorectal cancer in China: a meta-analysis of 29 trials involving 2,610 patients. *Oncotarget*. 2017;8(28):45164–45177. doi:10.18632/oncotarget.16665
- Lee JH, Lee JH, Lim YS, et al. Adjuvant immunotherapy with autologous cytokine-induced killer cells for hepatocellular carcinoma. *Gastroenterology*. 2015;148(7):1383–91 e6. doi:10.1053/j.gastro.2015.02.055
- Jiang J, Shen Y, Wu C, et al. Increasing the frequency of CIK cells adoptive immunotherapy may decrease risk of death in gastric cancer patients. *World J Gastroenterol*. 2010;16(48):6155–6162. doi:10.3748/wjg.v16.i48.6155
- Kirkwood J. Cancer immunotherapy: the interferon-alpha experience. *Semin Oncol*. 2002;29(3 Suppl 7):18–26. doi:10.1053/sonc.2002.33078
- Garbe C, Eigentler TK. Diagnosis and treatment of cutaneous melanoma: state of the art 2006. *Melanoma Res*. 2007;17(2):117–127. doi:10.1097/CMR.0b013e328042bb36
- Swann JB, Hayakawa Y, Zerafa N, et al. Type I IFN contributes to NK cell homeostasis, activation, and antitumor function. *J Immunol*. 2007;178(12):7540–7549. doi:10.4049/jimmunol.178.12.7540
- Brinkmann V, Geiger T, Alkan S, Heusser CH. Interferon alpha increases the frequency of interferon gamma-producing human CD4+ T cells. *J Exp Med*. 1993;178(5):1655–1663. doi:10.1084/jem.178.5.1655
- Liu W, Yang H, Hsu C, et al. Pegylated IFN-alpha suppresses hepatitis C virus by promoting the DAPK-mTOR pathway. *Proc Natl Acad Sci U S A*. 2016;113(51):14799–14804. doi:10.1073/pnas.1618517114
- Nishikawa M, Ogawa K, Umeki Y, et al. Injectable, self-gelling, biodegradable, and immunomodulatory DNA hydrogel for antigen delivery. *J Control Release*. 2014;180:25–32. doi:10.1016/j.jconrel.2014.02.001
- Umeki Y, Saito M, Kusamori K, et al. Combined encapsulation of a tumor antigen and immune cells using a self-assembling immunostimulatory DNA hydrogel to enhance antigen-specific tumor immunity. *J Control Release*. 2018;288:189–198. doi:10.1016/j.jconrel.2014.02.001
- Wang Y, Liu Z, Yuan H, et al. The reciprocity between radiotherapy and cancer immunotherapy. *Clin Cancer Res*. 2019;25(6):1709–1717. doi:10.1158/1078-0432.CCR-18-2581
- Galluzzi L, Chan TA, Kroemer G, et al. The hallmarks of successful anticancer immunotherapy. *Sci Transl Med*. 2018;10(459):459. doi:10.1126/scitranslmed.aat7807
- Ozpisgin OM, Zhang L, Li J. Immune targets in the tumor microenvironment treated by radiotherapy. *Theranostics*. 2019;9(5):1215–1231. doi:10.7150/thno.32648
- Binnewies M, Roberts EW, Kersten K, et al. Understanding the tumor immune microenvironment (TIME) for effective therapy. *Nat Med*. 2018;24(5):541–550. doi:10.1038/s41591-018-0014-x
- Klug F, Prakash H, Huber PE, et al. Low-dose irradiation programs macrophage differentiation to an iNOS(+)/M1 phenotype that orchestrates effective T cell immunotherapy. *Cancer Cell*. 2013;24(5):589–602. doi:10.1016/j.ccr.2013.09.014
- Du J, Su S, Li H, et al. Low dose irradiation increases adoptive cytotoxic T lymphocyte migration in gastric cancer. *Exp Ther Med*. 2017;14(6):5711–5716. doi:10.3892/etm.2017.5305
- Hoo SP, Sarvi F, Li WH, et al. Thermoresponsive cellulosic hydrogels with cell-releasing behavior. *ACS Appl Mater Interfaces*. 2013;5(12):5592–5600. doi:10.1021/am4009133
- Dimatteo R, Darling NJ, Segura T. In situ forming injectable hydrogels for drug delivery and wound repair. *Adv Drug Deliv Rev*. 2018;127:167–184. doi:10.1016/j.addr.2018.03.007
- Shao Y, Sun ZY, Wang Y, et al. Designable immune therapeutical vaccine system based on DNA supramolecular hydrogels. *ACS Appl Mater Interfaces*. 2018;10(11):9310–9314. doi:10.1021/acsami.8b00312
- Song H, Huang P, Niu J, et al. Injectable polypeptide hydrogel for dual-delivery of antigen and TLR3 agonist to modulate dendritic cells in vivo and enhance potent cytotoxic T-lymphocyte response against melanoma. *Biomaterials*. 2018;159:119–129. doi:10.1016/j.biomaterials.2018.01.004
- Weissenborn E, Braunschweig B. Hydroxypropyl cellulose as a green polymer for thermo-responsive aqueous foams. *Soft Matter*. 2019;15(13):2876–2883. doi:10.1039/c9sm00093c
- Xu K, Lee F, Gao SJ, et al. Injectable hyaluronic acid-tyramine hydrogels incorporating interferon-alpha2a for liver cancer therapy. *J Control Release*. 2013;166(3):203–210. doi:10.1016/j.jconrel.2013.01.008
- Tian L, Goldstein A, Wang H, et al. Mutual regulation of tumour vessel normalization and immunostimulatory reprogramming. *Nature*. 2017;544(7649):250–254. doi:10.1038/nature21724
- Ding N, Zou Z, Sha H, et al. iRGD synergizes with PD-1 knockout immunotherapy by enhancing lymphocyte infiltration in gastric cancer. *Nat Commun*. 2019;10(1):1336. doi:10.1038/s41467-019-09296-6
- Olioso P, Giancola R, Di Riti M, et al. Immunotherapy with cytokine induced killer cells in solid and hematopoietic tumours: a pilot clinical trial. *Hematol Oncol*. 2009;27(3):130–139. doi:10.1002/hon.886
- Dong Y, Jin G, Hong Y, et al. Engineering the cell microenvironment using novel photoresponsive hydrogels. *ACS Appl Mater Interfaces*. 2018;10(15):12374–12389. doi:10.1021/acsami.7b17751
- Choi JR, Yon KW, Choi JY, et al. Recent advances in photo-cross-linkable hydrogels for biomedical applications. *BioTechniques*. 2019;66(1):40–53. doi:10.2144/btn-2018-0083
- Dong Y, Jin G, Hong Y, et al. Engineered photo-responsive materials for near-infrared-triggered drug delivery. *J Ind Eng Chem*. 2015;31:15–25. doi:10.1016/j.jiec.2015.07.016

38. Joyce JA, Fearon DT. T cell exclusion, immune privilege, and the tumor microenvironment. *Science*. 2015;348(6230):74–80. doi:10.1126/science.aaa6204
39. Chan JK, Hamilton CA, Cheung MK, et al. Enhanced killing of primary ovarian cancer by retargeting autologous cytokine-induced killer cells with bispecific antibodies: a preclinical study. *Clin Cancer Res*. 2016;12(6):1859–1867. doi:10.1158/1078-0432.CCR-05-2019
40. Zuo S, Wen Y, Panha H, et al. Modification of cytokine-induced killer cells with folate receptor alpha (FRalpha)-specific chimeric antigen receptors enhances their antitumor immunity toward FRalpha-positive ovarian cancers. *Mol Immunol*. 2017;85:293–304. doi:10.1016/j.molimm.2017.03.017

International Journal of Nanomedicine

Dovepress

Publish your work in this journal

The International Journal of Nanomedicine is an international, peer-reviewed journal focusing on the application of nanotechnology in diagnostics, therapeutics, and drug delivery systems throughout the biomedical field. This journal is indexed on PubMed Central, MedLine, CAS, SciSearch®, Current Contents®/Clinical Medicine,

Journal Citation Reports/Science Edition, EMBase, Scopus and the Elsevier Bibliographic databases. The manuscript management system is completely online and includes a very quick and fair peer-review system, which is all easy to use. Visit <http://www.dovepress.com/testimonials.php> to read real quotes from published authors.

Submit your manuscript here: <https://www.dovepress.com/international-journal-of-nanomedicine-journal>